# New method for analyzing the synchronization of synaptic input and spike output in neural systems

A. N. Burkitt and G. M. Clark
The Bionic Ear Institute,
384–388 Albert Street,
East Melbourne, Vic 3002, Australia
email:burkitta@mail.medoto.unimelb.edu.au

*ABSTRACT*

*We present a new technique for analyzing the probability distribution of output spikes for the integrate and fire model. Using this method we investigate models with arbitrary synaptic response functions and the results, which are compared with numerical simulations, are exact in the limit of a large number of small amplitude inputs. We apply this method to the synchronization problem, in which the relationship between the spread in arrival times of the inputs (the temporal jitter of the synaptic input) and the resultant spread in the times at which the output spikes are generated (output jitter) is analyzed. The results indicate that the ratio of the output jitter to the input jitter is consistently less than one and that it decreases for increasing numbers of inputs, in agreement with earlier studies. We identify the variation in the spike generating thresholds of the neurons and the variation in the number of active inputs as being important factors that determine the timing jitter in layered networks, in addition to those identified previously.*

## 1. Introduction

In this paper we present a new technique for analyzing the integrate and fire model [1, 2], in which the incoming postsynaptic potentials (PSPs) generate an action potential (spike) when their sum reaches a threshold, in the presence of stochastic synaptic input (see [3, 4] for a review of stochastic processes in neuroscience). The technique allows us to include incoming excitatory and inhibitory postsynaptic potentials (EPSPs and IPSPs respectively) that have arbitrary time courses, so that we can incorporate such physiological features as the decay of the membrane potential and rise time of the synaptic current. A central part of the analysis is a Taylor's series expansion in the amplitude of the incoming postsynaptic potential. Only the linear and quadratic terms are retained and consequently the technique is accurate in the limit of small amplitude EPSPs, which necessitates a large number of inputs for the potential to reach threshold. This small amplitude expansion enables us to calculate the probability density function of the membrane potential reaching threshold and the probability density of output spikes, as discussed in the next section.

In the study described here this new technique is used to examine the temporal relationship between the synaptic input and spike output of neurons for the situation where the input is synchronized within some narrow time interval, which is characterized by the standard deviation in the time of arrival (denoted as the input jitter). The situation in which the inputs are Poisson distributed can also be analyzed using similar techniques [5].

The principal reason that synchrony of neuronal firing in groups of neurons has attracted such attention is the belief that it provides an efficient method to increase the reliability of responses: a neuron that receives many inputs simultaneously is much more likely to generate a spike than one that either receives fewer inputs or the same number of inputs distributed over a longer time interval. The importance of synchronization for neuronal information processing is on the level of *groups* of neurons, such as proposed by the *synfire* model [6, 7] in which synchronized input to a group of neurons is propagated to successive groups of neurons, called a *synfire chain*. Synchronization provides the possibility of establishing relationships between neuronal responses [8], such as grouping together (binding) neurons that respond to the same features of a stimulus [9]. By establishing a synchronous firing pattern the grouping of neurons is resistant to amplitude fluctuations and several such assemblies of neurons can coexist. Such a mechanism would provide a neurophysiological correlate to the cognitive phenomena of scene segmentation and feature linking [10, 11]. Increasing the likelihood of firing for neurons associated with a particular feature enables the selection of responses for further processing.

## 2. New method for the analysis of integrate and fire neurons

We analyze an integrate and fire neuron with a large number $N$ of incoming EPSPs, so that the resultant membrane potential at time $t$ is given by the sum of the inputs

$$V(t) = v_0 \; + \; a \sum_{k}^{N} u(t - t_k) \tag{1}$$

where $v_0$ is the resting membrane potential, $N$ is the number of active inputs (i.e., number of afferent fibers which actually contribute a postsynaptic input) each of amplitude $a$, and $t_k$ is the time of arrival of the EPSP from the $k^{th}$ fiber, which has a time-dependence that is described by the synaptic response function $u(t)$. We wish to calculate the relationship between the time of arrival of the inputs, characterized by a Gaussian distribution with mean $t_k = 0$ and standard deviation $\sigma_{\rm in}$ (also called input jitter), and the spread in the timing of the output distribution of spikes $\sigma_{\rm out}$ (the output jitter).

### 2.1. The probability distribution

In order to calculate the probability that a spike is generated, we first calculate the probability distribution of the sum $V(t)$ of the incoming EPSPs, equation(1). The probability that this potential $V(t)$ exceeds the value $v$ at time $t$ is evaluated by considering the proportion of cases for which this is true. This is given by integrating over the distribution of arrival times for all incoming EPSPs

$$\begin{aligned}&\Pr\{V(t) \geq v \,|\, V(-\infty) = v_0\} = \\ &\qquad \prod_{k}^{N} \int_{-\infty}^{\infty} dt_k \; p(t_k) \; H(V(t) - v)\end{aligned} \tag{2}$$

where we assume that the membrane potential is at its resting value $v_0$ before the arrival of the EPSPs (i.e., $V(-\infty) = v_0$). The Heaviside step function $H(x)$ gives a contribution of one for $V(t) \geq v$ and zero otherwise. Using an integral representation of the Heaviside step function

$$H(z - z_0) = \int_{z_0}^{\infty} \frac{d\lambda}{2\pi} \int_{-\infty}^{\infty} dx \; \exp\{i\, x\, (\lambda \, - z)\}. \tag{3}$$

the contributions from the incoming fibers can be treated independently. Since each incoming fiber has the same distribution of arrival times of EPSPs, the above probability may be written as

$$\begin{aligned}&\Pr\{V(t) \geq v \,|\, V(-\infty) = v_0\} = \\ &\int_{v - v_0}^{\infty} \frac{d\lambda}{2\pi} \int_{-\infty}^{\infty} dx \; \exp\{i\, x\, \lambda\} \; [F(x,t)]^N\end{aligned} \tag{4}$$

where the function $F(x,t)$ is given by

$$F(x,t) = \int_{-\infty}^{\infty} dt' \; p(t') \; \exp\{-i\, x\, a\, u(t - t')\} \tag{5}$$

We consider the situation where the number of inputs $N$ is large and each of the inputs has an amplitude $a$ that is small (in comparison to the threshold). Expanding the exponential to second order in the amplitude $a$ of the EPSP and neglecting higher order terms,

$$F(x,t) \approx 1 - i\, x\, a\, D(t) - \frac{x^2\, a^2}{2} E(t) \tag{6}$$

where

$$\begin{aligned} D(t) &= \int_{-\infty}^{t} dt' \; p(t') \; u(t - t') \\ E(t) &= \int_{-\infty}^{t} dt' \; p(t') \; u^2(t - t'). \end{aligned} \tag{7}$$

The probability distribution can then be evaluated (see [12] for details)

$$\begin{aligned}&\Pr\{V(t) \geq v \,|\, V(-\infty) = v_0\} = \\ &\qquad \frac{1}{2}\left[1 - \operatorname{erf}\left(\frac{v - v_0 - \Lambda(t)}{\sqrt{2\,\Gamma(t)}}\right)\right]\end{aligned} \tag{8}$$

with

$$\begin{aligned} \Lambda(t) &= N\, a\, D(t) \\ \Gamma(t) &= N\, a^2\, (E(t) - D^2(t)). \end{aligned} \tag{9}$$

The probability density function of $V(t)$ is given by

$$\begin{aligned} p(v,t|v_0) &= \frac{d}{dv} \Pr\{V(t) \leq v \,|\, V(-\infty) = v_0\} \\ &= \frac{1}{\sqrt{2\,\pi\,\Gamma(t)}} \exp\left\{-\frac{(v - v_0 - \Lambda(t))^2}{2\,\Gamma(t)}\right\}. \end{aligned}$$

In the following analysis the threshold will be expressed in terms of the *threshold ratio* $R$, which is ratio of the threshold $V_{\rm th} = \theta + v_0$ to the maximum possible value $V_{\rm max}$ of $V(t)$ (i.e., if all contributions arrived simultaneously), both with respect to the resting potential $v_0$,

$$R = \frac{V_{\rm th} - v_0}{V_{\rm max} - v_0} = \frac{\theta}{N a} \tag{10}$$

where there are $N$ contributions each of amplitude $a$. We choose the units of voltage to be set by the threshold, $\theta = 1$. The expansion of equation(6) to second order in the amplitude $a$ of the individual EPSPs is an approximation that is good for values of $a$ that are small in comparison to the threshold, which is frequently the case in biological neural systems.

### 2.2. Probability density of output spikes

The probability density of the output spikes is the density of the potential $V(t)$ reaching the threshold $V_{\rm th}$ for the *first* time, called the first-passage time to threshold. This may be obtained from the renewal-like equation (for $v > V_{\mathrm{th}}$)

$$p(v,t|v_0) = \int_{-\infty}^{t} dt'\; f_\theta(t')\; p(v,t|V_{\mathrm{th}},t',v_0) \quad (11)$$

where the function $p(v_2,t_2|v_1,t_1,v_0)$ is the conditional probability density of $V(t)$ taking the value $v_2$ at time $t_2$ given that it had taken the value $v_1$ at time $t_1$ (and also had the value $v_0$ at time $-\infty$). The conditional probability density may be evaluated via the relation (Bayes' theorem)

$$p(v_2,t_2|v_1,t_1,v_0) = \frac{p(v_2,t_2,v_1,t_1|v_0)}{p(v_1,t_1|v_0)}. \quad (12)$$

The joint probability density $p(v_2,t_2,v_1,t_1|v_0)$ is evaluated in a similar way to the probability density (see [12] for details)

$$p(v_2,t_2\,|\,v_1,t_1,v_0) = \frac{1}{\sqrt{2\pi\gamma}} \times \exp\left\{-\frac{[(v_2-v_0-\Lambda(t_2)-\kappa(v_1-v_0-\Lambda(t_1))]^2}{2\,\gamma}\right\} \quad (13)$$

where

$$\begin{aligned}
\gamma(t_2,t_1) &= \Gamma(t_2) - \frac{\chi^2(t_2,t_1)}{\Gamma(t_1)} \\
\kappa(t_2,t_1) &= \frac{\chi(t_2,t_1)}{\Gamma(t_1)} \quad (14)\\
\chi(t_2,t_1) &= N\,a^2\,[G(t_2,t_1) - D(t_2)D(t_1)]
\end{aligned}$$

and

$$G(t_2,t_1) = \int_{-\infty}^{t_1} dt'\; p(t')\; u(t_2-t')\; u(t_1-t'). \quad (15)$$

The first passage-time density may be parameterized as a Gaussian distribution with probability $\rho$ of a spike being produced, average time of the first threshold crossing $t_f$ (i.e., time of spike production relative to the distribution of inputs), and jitter of the output distribution of spikes $\sigma_{\mathrm{out}}$. Equation(11), which defines the probability density of output spikes, is in general difficult to solve analytically. However it is straightforward to solve for the parameters $\rho$, $t_f$ and $\sigma_{\mathrm{out}}$ using the Newton-Raphson method for nonlinear systems of equations (see, for example, [13]).

## 3. Synchronization in integrate and fire neural models

### 3.1. Perfect integrator model

Within the family of integrate and fire models the simplest case to consider is that of the perfect integrator, in which there is no decay of the potential with time. Although this is an unphysiological assumption, it may provide a reasonable approximation for situations in which the integration occurs over a time scale much shorter than the decay constant. The model has been extensively studied because it is more amenable to analytical solution than the leaky integrate and fire model.

In this leakless model the probability density of output spikes $f_\theta(t)$ may be solved exactly by considering the distribution of arrival times of the contributing EPSPs as a combinatorial problem. If the threshold is crossed with the arrival of the $M^{\mathrm{th}}$ input, then the resulting distribution of the output spikes is

$$f_M(t) = \frac{N!\,M}{M!\,(N-M)!}\;\; p(t)\,\beta^{M-1}(t)\;(1-\beta(t))^{N-M} \quad (16)$$

where $p(t)$ is the Gaussian probability distribution of incoming EPSPs and $\beta(t)$ is given by

$$\beta(t) = \int_{-\infty}^{t} dt'\, p(t') \;= \frac{1}{2}\left[1+\mathrm{erf}\left(\frac{t}{\sqrt{2}\,\sigma_{\mathrm{in}}}\right)\right] \quad (17)$$

This exact result is compared with the result obtained by our new analytical method. Since there is no inherent unit of time in this model, we choose the time scale to be set by $\sigma_{\mathrm{in}} = 1$. The results for the perfect integrator model are shown in Figure 1 for a number of inputs $N$ in the range 10 to 800, and a range of threshold values $R$. The dotted lines connect the exact results of equation(16) and the solid lines connect the results of the numerical solution to equation(11). These results clearly show that the output jitter $\sigma_{\mathrm{out}}$ decreases with increasing $N$, and that it is substantially less than the input jitter ($\sigma_{\mathrm{in}} = 1$) over the whole range of values of $N$. The results from the analytical expression show extremely good agreement with the exact results over a wide range of thresholds for 50 inputs, and the difference diminishes for increasing $N$ such that the error is less than 1% for 100 inputs. For $N \geq 200$ the analytical results agree with the exact results over the range of threshold ratios investigated. For large numbers of inputs the exact output spike distribution, equation(16), becomes Gaussian, but for small $N$ there will be corrections to the Gaussian parameterization, which will contribute to the differences between the exact and the analytic expressions evident in Figure 1. In addition, for a fixed number of inputs the small amplitude approximation will be least accurate for small threshold ratios (equation 10). General considerations indicate that very low threshold ratio neurons tend to have high levels of spontaneous activity, whereas very high ratio neurons tend to have very low activity and be difficult to excite. Biological neural systems would therefore be expected to function within the broad intermediate threshold region, where the technique presented here provides an accurate approximation for large numbers of input neurons.

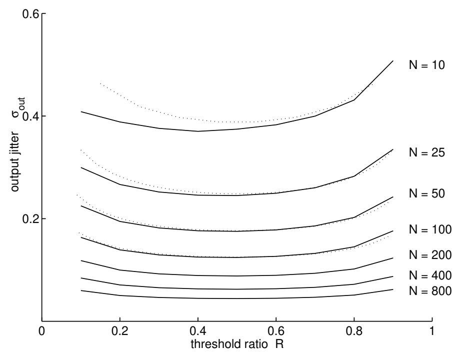


Fig. 1: Results for the perfect integrator model. The dependence of the output jitter $\sigma_{\text{out}}$ upon the threshold for a range of afferent fibers $N$ is shown, with $\sigma_{\text{in}} = 1$. The threshold ratio $R$ is given by $\theta / Na$. The solid lines connect the results of the solution to equation(11) and the dotted lines connect the results of the exact solution (equation 16). The two sets of results are indistinguishable for $N \geq 200$.

### 3.2. Stein model

Although the perfect integrator model may be adequate to explain some phenomena, it is nevertheless necessary in general to consider the effect of the leakage of the potential across the membrane, as first analyzed by Stein [14]. In the Stein model the membrane potential has a discontinuous jump of amplitude $a$ upon the arrival of an EPSP and then decays exponentially with time constant $\tau$ between inputs.

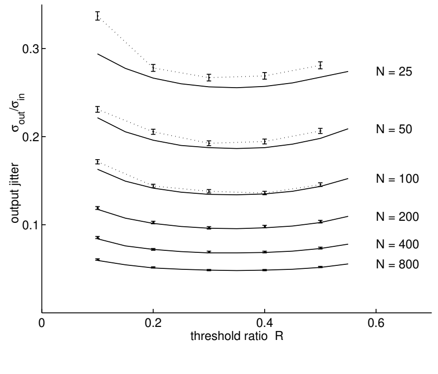


Fig. 2: The relative output jitter $\sigma_{\text{out}}/\sigma_{\text{in}}$ for the Stein model with various numbers of input EPSPs and threshold ratios $R$. The jitter of the input $\sigma_{\text{in}}$ is 0.2 in units of the membrane time constant ($\tau$=1). The solid line shows the value obtained from the solution of equation(11) and the data points connected by the dotted lines are each the result of 10,000 numerical simulations.

The relative output jitter is plotted in Figure 2 for $\sigma_{\text{in}} = 0.2$ and a range of input values $N$ and threshold ratios $R$ (defined as before by equation 10). The renewal-like equation(11) for the output spike density was solved numerically, using the Newton-Raphson method as before, for a range of threshold ratios $R = 0.10, 0.15, ..., 0.55$, and the results are connected by the solid lines. Also plotted are the results of a number of numerical simulations, each point representing the average over 10,000 trials. The error bars give the standard deviation over the trials, and the results for each value of $N$ are connected by a dashed line (for the larger values of $N$ the error bars are roughly the width of the lines and therefore barely discernable). The relative output jitter is clearly substantially less than the input jitter over the whole range of inputs and threshold ratios investigated. The results from the analytical expression derived here are very accurate for large numbers of inputs $N$, as shown by their closeness with the results of the numerical simulations. As before, the expected error of the method presented here decreases as the number of inputs $N$ increases and the amplitude $a$ of each individual contribution decreases.

## 4. Discussion and Conclusions

In this study we have presented a new method for analyzing integrate and fire neurons with a large number of small amplitude inputs. This technique allows the analysis of models with arbitrary synaptic response functions, and in particular models that incorporate both leakage (the Stein model, analyzed here) and a finite rise time of the postsynaptic potential (analyzed in [12]), which has previously been possible only in very restricted cases. The method has been used to examine the question of the relationship between the temporal dispersion of synchronized inputs and the resulting jitter of the spikes that are generated. The results are compared with the exact solution for the perfect integrator model and with numerical simulations for the Stein model. The results of the analysis of the relationship between the input jitter and the output jitter provides clear support for earlier studies [15, 16, 17] showing that the jitter of the spike output is much less than the jitter on the incoming PSPs, i.e., that the temporal dispersion of the output spikes is less than the temporal dispersion of the inputs, $\sigma_{\text{out}} < \sigma_{\text{in}}$, over a wide range of physiologically realistic conditions. Such a reduction in the temporal jitter has indeed been observed experimentally in the anteroventral cochlear nucleus [18].

In a cascade of neurons there are a number of sources of variability, in addition to the jitter of the inputs, that determine the stability of the neuronal firing pattern [19] and prevent the output jitter from converging to zero. Maršálek *et al.* [17] identified two important factors that introduce timing variability to the arriving PSPs: (i) the delay due to different spike propagation times, and (ii) the jitter associated with the synapses. Another important factor is the variation in the spiking thresholds of the neurons, which will cause different neurons to spike at different relative times, as we discuss further in [12]. Neurons with different threshold ratios have substantial differences in the average times at which spikes are generated. Consequently variations of the spiking threshold over a layer of neurons will cause variations in the relative timing of the output spikes produced by the population of neurons. In such a layered network this variation in the timing of the spikes from the previous layer will represent jitter on the inputs to the subsequent layer, which is additional to the inherent jitter associated with the production of the spikes.

We have studied here an idealized situation in which spontaneous activity is neglected, and investigations are currently underway to analyze the integrate and fire model with Poisson distributed inputs using methods similar to those presented above [5]. This will then enable the study of more complex systems of synaptic inputs involving partial synchronization together with spontaneous activity or systematic phase delays, such as occur in auditory nerve fibers excited by a travelling wave along the basilar membrane of the inner ear [20].

## Acknowledgments

This work was funded by the Cooperative Research Centre for Cochlear Implant, Speech & Hearing Research.

### References

[1] L. Lapicque. Recherches quantitatives sur l'excitation electrique des nerfs traitee comme une polarization. *J. Physiol. (Paris)*, 9:620–635, 1907.

[2] H. C. Tuckwell. *Introduction to Theoretical Neurobiology: Volume 1, Linear Cable Theory and Dendritic Structure.* Cambridge University Press, Cambridge, 1988.

[3] H. C. Tuckwell. *Introduction to Theoretical Neurobiology: Volume 2, Nonlinear and Stochastic Theories.* Cambridge University Press, Cambridge, 1988.

[4] H. C. Tuckwell. *Stochastic Processes in the Neurosciences.* Society for Industrial and Applied Mathematics, Philadelphia, 1989.

[5] A. N. Burkitt and G. M. Clark. Manuscript in preparation, 1997.

[6] M. Abeles. *Local Cortical Circuits: An Electrophysiological Study.* Springer, Berlin, 1982.

[7] M. Abeles. *Corticonics: Neural Circuits of the Cerebral Cortex.* Cambridge University Press, New York, 1991.

[8] M. Usher, H. G. Schuster, and E. Niebur. Dynamics of populations of integrate-and-fire neurons, partial synchronizaton and memory. *Neural Comp.*, 5:570–586, 1993.

[9] A. K. Engel, P. König, A. K. Kreiter, T. B. Schillen, and W. Singer. Temporal coding in the visual cortex: New vistas on integration in the nervous system. *Trends Neurosci.*, 15:218–226, 1992.

[10] R. Eckhorn, R. Bauer, W. Jordan, M. Brosch, W. Kruse, M. Munk, and H. J. Reitboeck. Coherent oscillations: A mechanism of feature linking in the visual cortex? *Biol. Cybern*, 60:121–130, 1988.

[11] A. K. Engel, P. König, and W. Singer. Direct physiological evidence for scene segmentation by temporal coding. *Proc. Natl. Acad. Sci. USA*, 88:9136–9140, 1991.

[12] A. N. Burkitt and G. M. Clark. Analysis of the synchronization of synaptic input and spike output in neural systems, 1997. Submitted for publication.

[13] W. H. Press, B. P. Flannery, S. A. Teukolsky, and W. T. Vetterling. *Numerical Recipes in Fortran: The Art of Scientific Computing.* Cambridge University Press, Cambridge, 1992.

[14] R. B. Stein. A theoretical analysis of neuronal variability. *Biophys. J.*, 5:173–194, 1965.

[15] O. Bernander, C. Koch, and M. Usher. The effect of synchronized inputs at the single neuron level. *Neural Comp.*, 6:622–641, 1994.

[16] M. Diesmann, M. O. Gewaltig, and A. Aertsen. Characterization of synfire activity by propagating 'pulse packets'. In J. Bower, editor, *Computational Neuroscience: Trends in Research*, pages 59–64, San Diego, 1996. Academic Press.

[17] P. Maršálek, C. Koch, and J. Maunsell. On the relationship between synaptic input and spike output jitter in individual neurons. *Proc. Natl. Acad. Sci. USA*, 94:735–740, 1997.

[18] P. X. Joris, L. H. Carney, P. H. Smith, and T. C. T. Yin. Enhancement of neural synchronization in the anteroventral cochlear nucleus. I.responses to tones at the characteristic frequency. *J. Neurophysiol.*, 71:1022–1036, 1994.

[19] W. Gerstner and J. L. van Hemmen. What matters in neuronal locking? *Neural Comp.*, 8:1653–1676, 1996.

[20] I. C. Bruce, L. S. Irlicht, and G. M. Clark. A mathematical analysis of spatiotemporal summation of auditory nerve fibers, 1997. Submitted to Information Sciences Applications.